A quasi-droplet optofluidic ring resonator laser using a micro-bubble

Wonsuk Lee,[1,2] Yuze Sun,[1] Hao Li,[1,3] Karthik Reddy,[1,2] Misha Sumetsky,[4] and Xudong Fan[1,a)]

[1]*Department of Biomedical Engineering, University of Michigan, 1101 Beal Ave., Ann Arbor, Michigan 48109, USA*
[2]*Department of Electrical Engineering and Computer Science, University of Michigan, 1301 Beal Ave., Ann Arbor, Michigan 48109, USA*
[3]*Key Laboratory for Micro and Nano Photonic Structures (Ministry of Education), Department of Optical Science and Engineering, Fudan University, Shanghai 200433, People's Republic of China*
[4]*OFS Laboratories, 19 Schoolhouse Road, Somerset, New Jersey 08873, USA*

(Received 30 June 2011; accepted 5 August 2011; published online 29 August 2011)

Optofluidic ring resonator lasers based on micro-bubbles filled with liquid gain medium are demonstrated. Due to the sub-micron wall thickness of the micro-bubble, significant amount of the electric field resides inside the liquid. Consequently, micro-bubbles mimic the droplets in air that have 3-dimensional optical confinement, extremely high Q-factors, and versatility in handling liquids of different refractive index. Furthermore, they enable repetitive interrogation and easy directional laser emission out-coupling without evaporation or size/shape variations. The laser using Rhodamine 6G in methanol is achieved with a threshold of 300 nJ/mm^2 and 5.3 μJ/mm^2 for 1 mM and 10 μM in concentration, respectively. © *2011 American Institute of Physics*. [doi:10.1063/1.3629814]

Micro-droplets naturally integrate liquid and optical ring resonator and thus are of great interest in the development of optofluidic device.[1–3] The micro-droplet supports the whispering gallery modes (WGMs), which circulate along the droplet surface and provide optical feedback for the gain medium dissolved in the droplet to lase.[1] Micro-droplet lasers have been studied in 1980s and 1990s using free-falling or levitated droplets,[1,4,5] and recently using those formed on an ultra-hydrophobic surface.[6–8] They exhibit low lasing thresholds due to their extremely high Q-factors resulting from the smooth liquid-air interface and 3-dimensional light confinement, and are versatile in handling different liquids, in particular, water-based ones. However, those droplet lasers suffer from rapid liquid evaporation, lack of good control of size and shape, low efficiency of out-coupling into waveguiding components and bulky droplet generators, which significantly hinder the development of the droplet lasers into a practically useful device.

More recently, rapid generation of a large number of micro-droplets and subsequent demonstration of the corresponding droplet lasers have been achieved using microfluidics with two immiscible liquids.[9–11] While those designs partially solve the aforementioned problems by miniaturizing the device and preventing evaporation of the liquid, new concerns emerge. Since droplets are surrounded by the carrier liquid, the refractive index (RI) of the droplet should be larger than that of the carrier fluid, which imposes considerable limitations in liquid selection.[9–11] In addition, the low RI contrast between the droplet and the carrier liquid significantly deteriorates the Q-factor.[9] In particular, for water based droplets which are important for bio/chemical applications,[12–15] the RI contrast is so low that no laser emission is observed.[9] In addition, droplet size variation and shape deformation due to the perturbations during the droplet generation and composition change due to the gradual mixing with the carrier liquid make the lasing characteristics less consistent.[11] Finally, the laser emission collection remains inefficient as only the free-space coupling mechanism can be used.

In this letter, we fabricate, characterize, and demonstrate a quasi-droplet optofluidic ring resonator (OFRR) laser based on a fused silica micro-bubble with an extremely thin wall. The bubble is formed by pressurizing a glass capillary under CO_2 laser irradiation.[16,17] The wall thickness as thin as 560 nm is achieved. Consequently, when the bubble is filled with liquid, significant amount of the electric field of the WGM resides inside the liquid, thus making the composite micro-bubble and liquid system a quasi-droplet. The quasi-droplet laser has a number of advantages, as compared to the droplet laser discussed previously. (1) It mimics the droplet in air that provides excellent Q-factors and 3-dimensional light confinement; (2) It is as versatile as the droplet in air and is capable of handling liquid of any RI; (3) It enables repetitive interrogation without any problems in evaporation, size variation, or shape deformation; (4) Its laser emission can be easily out-coupled through a waveguide or tapered optical fiber in contact with the bubble.

The fabrication processes of the micro-bubble are adapted from our previous work.[16,17] First, we pre-etch a fused silica capillary, which has the outer diameter of 100 μm

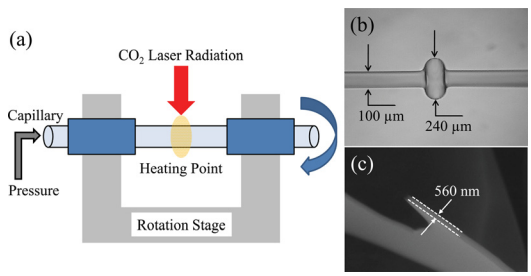

FIG. 1. (Color online) (a) Illustration of the setup for the micro-bubble fabrication. (b) Microscopic image of the micro-bubble made on the pre-etched capillary. (c) SEM image of the broken micro-bubble for measuring wall thickness. The thickness of the micro-bubble wall near the equator is 560 nm.

a)Electronic mail: xsfan@umich.edu.

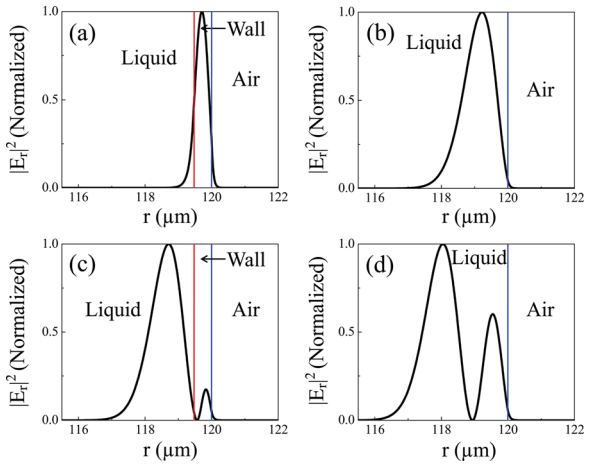

FIG. 2. (Color online) Normalized electric field distribution of the 1st ((a) and (b)) and 2nd ((c) and (d)) TM WGM in the radial direction in the micro-bubble ((a) and (c)) and the droplet ((b) and (d)). The radii of the micro-bubble and the droplet are both 120 μm, and the wall thickness of the micro-bubble is 560 nm, as illustrated by solid lines, respectively. Wavelength near 590 nm is used in the calculation and the micro-bubble is assumed to be a perfect hollow sphere filled with low index liquid (RI = 1.33).

after conventional drawing,[18,19] to obtain optimal wall thickness for the micro-bubble fabrication. After 5% aqueous hydrofluoric acid is flowed through the capillary for 2 h, the wall thickness of the capillary is approximately 4.8 μm. We then connect the pre-etched capillary to the rotation stage with epoxy, and the capillary is pressurized and rotated under CO_2 laser radiation, as illustrated in Fig. 1(a). The CO_2 laser is tightly focused into a spot of a few hundred micrometers in diameter, and a portion of the capillary heated by the laser is blown up to form the micro-bubble. Fig. 1(b) shows the microscopic image of the micro-bubble with an outer diameter of 240 μm. In order to characterize the wall thickness, we break the micro-bubble and exam it under a scanning electron microscope (SEM). As shown in Fig. 1(c), the micro-bubble has a wall as thin as 560 nm at its thinnest part (near the bubble equator). After the micro-bubble is formed on the capillary, fluidic channels are built at the both ends of capillary, enabling liquid to flow through the capillary and micro-bubble as well. Note that using the similar blowing technology, the dead-ended micro-bubble has also been demonstrated very recently.[20] However, the flow-through structure reported here makes liquid delivery and replacement much easier and is highly compatible with upstream and downstream micro-fluidics.

The fraction of energy residing inside the low-index liquid core surrounded by the glass WGM resonator increases as the wall thickness decreases.[21] Since the liquid gain medium of our quasi-droplet laser is inside the fused silica micro-bubble, the wall should be thin enough to push the electric field into the liquid core in order to provide sufficient optical feedback for lasing. Fig. 2 plots the calculated electric field radial distribution of the transverse magnetic (TM) WGM of a micro-bubble filled with low index liquid (RI = 1.33) and the corresponding liquid droplet of the same size, respectively. Although for the 1st order mode, only 9.6% of the WGM resides inside the liquid core in contrast to over 99% of energy confined in the droplet, the fractional energy inside the liquid becomes nearly the same for the 2nd (and higher) order mode (96% vs. 99%), suggesting that the micro-bubble is virtually a droplet for those modes.

The Q-factor of a perfectly shaped micro-bubble resonator filled with the liquid is limited mainly by the absorption of the liquid, since the fused silica absorption loss is nearly negligible. It can be estimated using a relation of $Q = 2\pi n/\eta\alpha\lambda$, where n, λ, α, and η are the effective RI, wavelength, attenuation coefficient of the liquid, and the fraction of energy residing inside the liquid core, respectively. For methanol and water, α is 5.9×10^{-4} cm^{-1} and 0.0035 cm^{-1} at 532 nm wavelength, respectively.[22] With $\eta = 0.96$, a Q-factor of our laser cavity of approximately 10^8 is achievable. Note that, while experimentally such a high Q-factor can be characterized more accurately with cavity ring-down spectroscopy in the time domain,[23] our previous studies in the spectral domain on the micro-bubble resonator fabricated using the same method showed a Q-factor exceeding 10^6 limited only by resolution of the spectrometer.[16,17]

To investigate lasing characteristics of our laser, we use Rhodamine 6G (R6G) dissolved in methanol, which has a RI (= 1.33) similar to that of water. We flow the R6G solution through the micro-bubble with a flow-rate of 0.1 μL/min. The micro-bubble is pumped by a 5 ns pulsed optical parametric oscillator at 532 nm. The lasing emission is then evanescently coupled out via a tapered optical fiber in contact with the micro-bubble and sent to a spectrometer (Horiba iHR550, resolution of 0.06 nm).

Fig. 3(a) shows the lasing spectrum of the quasi-droplet laser using 1 mM R6G solution, when the pump energy density is 2.6 $\mu J/mm^2$. In contrast, the previous work shows no laser observed for such low RI droplets generated using two immiscible liquids due to very low RI contrast.[9] The laser emission ranges from 580 to 600 nm, similar to what is observed in droplet lasers.[24] The peak intensity of the laser as a function of the pump energy density is plotted in Fig. 3(b). The curve shows that the lasing threshold is approximately 300 nJ/mm^2, one order of magnitude lower than other optofluidic lasers, indicative of a high Q-factor of our quasi-droplet and strong light-gain medium interaction. Note that, due to

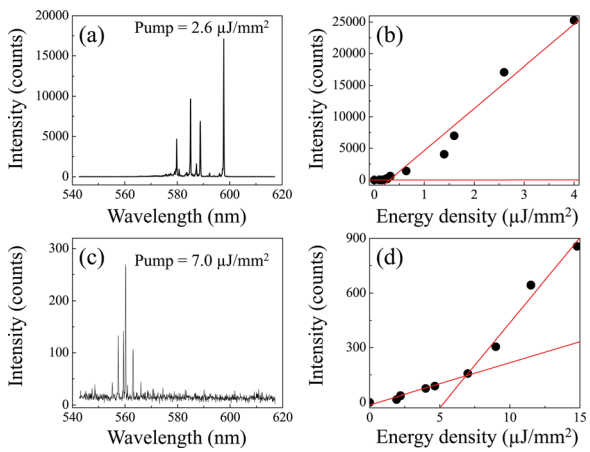

FIG. 3. (Color online) (a) Lasing spectrum of the quasi-droplet OFRR laser for 1 mM R6G in methanol. (b) Lasing threshold curve corresponding to (a). The threshold is approximately 300 nJ/mm^2. (c) Lasing spectrum of the same for 1 μM R6G in methanol. (d) Lasing threshold curve corresponding to (c). The threshold is 5.3 $\mu J/mm^2$. Solid lines in (b) and (d) are the linear fit for the dye emission below and above the lasing threshold.

the 3-dimensional light confinement, the number of the lasing peaks from the quasi-droplet OFRR laser is lower than that from a conventional micro-capillary based OFRR laser. These laser peaks emerge nearly simultaneously, as they have very similar lasing thresholds, as discussed previously.[25,26] When the concentration of R6G is reduced to 10 μM, we obtain the lasing spectrum as depicted in Fig. 3(c), under the pump energy density of 7.0 μJ/mm^2. Note that the lasing wavelength blue-shifts due to the decrease in dye absorption.[25,26] The corresponding lasing threshold curve is shown in Fig. 3(d) and shows that the threshold is increased to 5.3 μJ/mm^2, as expected.[25,26] As low concentrations of dye solution are particularly important for bio/chemical sensing and biomedical applications of the OFRR lasers, we further decrease the R6G concentration. Fig. 4 shows that the laser emission can still be achieved even with 1 μM R6G solution. The corresponding lasing threshold is estimated to be approximately 20 μJ/mm^2.

Since our quasi-droplet laser has an advantage in liquid delivery, the dye solution filling out the micro-bubble can be easily replaced, which enables tuning of the lasing wavelength. As we switch the dye from R6G to LDS722, we are able to obtain the shifted lasing emission ranging from 700 to 750 nm, as indicated in Fig. 5(a). The lasing threshold curve of 1 mM LDS722 laser is shown in Fig. 5(b), and the threshold of 0.52 μJ/mm^2 is obtained.

Moreover, the quasi-droplet laser mimics the droplet in the air, thus, it can handle the liquid gain medium of any RI, as expected previously. Fig. 5(c) presents the lasing spectrum of the quasi-droplet laser when quinoline (RI $\sim$ 1.626, larger than the RI of the wall) is used as a solvent to dissolve 1 mM R6G. The corresponding threshold is approximately 400 nJ/mm^2. Both the spectrum and the threshold are similar to those of the methanol laser with the same dye concentration [see Figs. 3(a) and 3(b)], suggesting that the fraction of the WGM interacting with the gain medium is similar, despite large RI difference between quinolone and methanol.

In conclusion, we have demonstrated a quasi-droplet OFRR laser utilizing a fused silica micro-bubble fabricated on the capillary by CO_2 laser heating and blowing. The laser shows a very low lasing threshold due to a high Q-factor and strong light-matter interaction of the micro-bubble. Lasing is also achieved for a dye concentration as low as 1 μM. Furthermore, our quasi-droplet laser can utilize a dye solution of any RI, thanks to an extremely thin wall of the micro-bubble. Finally, the quasi-droplet laser can be directionally out-coupled into a waveguide or fiber and can be interrogated repetitively, thus overcoming the problems associated with the free-falling droplets or the droplets generated via immiscible solutions.

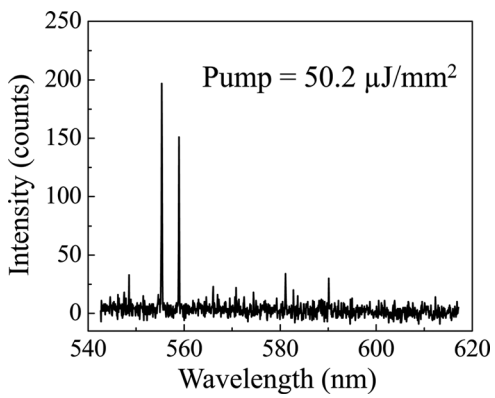

FIG. 4. Lasing spectrum of the quasi-droplet laser with 1 μM R6G.

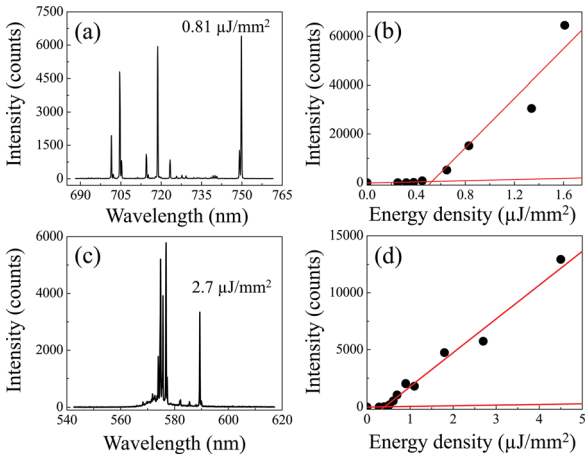

FIG. 5. (Color online) (a) Lasing spectrum of the quasi-droplet OFRR laser when 1 mM LDS722 dye dissolved in methanol is flowed through the micro-bubble. The pump energy density is 0.81 μJ/mm^2. (b) Corresponding threshold curve. The threshold is 0.52 μJ/mm^2. (c) Lasing spectrum of the same when 1 mM R6G dye dissolved in quinoline is flowed through the micro-bubble. The pump energy density is 2.7 μJ/mm^2. (d) Corresponding threshold curve. The threshold is approximately 400 nJ/mm^2. Solid lines in (b) and (d) are the linear fit for the dye emission below and above the lasing threshold.

W.L. and Y.S. contribute equally to this paper. The work is supported by the NSF under ECCS 1045621 and CBET 1037097.

[1]R. K. Chang and A. J. Campillo, *Optical Processes in Microcavities* (World Scientific, Singapore, 1996).
[2]Z. Li and D. Psaltis, Microfluid. Nanofluid. **4**, 145 (2008).
[3]Y. Zuta, I. Goykhman, B. Desiatov, and U. Levy, Opt. Express **18**, 24762 (2010).
[4]G. Chena, M. M. Mazumdera, R. K. Changa, J. C. Swindalb, and W. P. Acker, Prog. Energy Combust. Sci. **22**, 163 (1996).
[5]H.-B. Lin, J. D. Eversole, and A. J. Campillo, J. Opt. Soc. Am. B **9**, 43 (1992).
[6]A. Kiraz, A. Sennaroglu, S. Doganay, M. A. Dundar, A. Kurt, H. Kalaycıoglu, and A. L. Demirel, Opt. Commun. **276**, 145 (2007).
[7]A. Sennaroglu, A. Kiraz, M. A. Dündar, A. Kurt, and A. L. Demirel, Opt. Lett. **32**, 1297 (2007).
[8]M. Hossein-Zadeh and K. J. Vahala, Opt. Express **14**, 10800 (2006).
[9]M. Tanyeri, R. Perron, and I. M. Kennedy, Opt. Lett. **32**, 2529 (2007).
[10]S. K. Y. Tang, Z. Li, A. R. Abate, J. J. Agresti, D. A. Weitz, D. Psaltis, and G. M. Whitesides, Lab Chip **9**, 2767 (2009).
[11]S. K. Y. Tang, R. Derda, Q. Quan, M. Lončar, and G. M. Whitesides, Opt. Express **19**, 2204 (2011).
[12]S.-Y. Teh, R. Lin, L.-H. Hung, and A. P. Lee, Lab Chip **8**, 198 (2008).
[13]D. T. Chiu and R. M. Lorenz, Acc. Chem. Res. **42**, 649 (2009).
[14]Y. Sun, S. I. Shopova, C.-S. Wu, S. Arnold, and X. Fan, Proc. Natl. Acad. Sci. U.S.A. **107**, 16039 (2010).
[15]Y. Sun and X. Fan, in *CLEO/QELS* (Optical Society of America (OSA), Baltimore, MD, 2011), p. CWL6.
[16]M. Sumetsky, Y. Dulashko, and R. W. Windeler, Opt. Lett. **35**, 898 (2010).
[17]M. Sumetsky, Y. Dulashko, and R. W. Windeler, Opt. Lett. **35**, 1866 (2010).
[18]I. M. White, H. Oveys, and X. Fan, Opt. Lett. **31**, 1319 (2006).
[19]S. I. Shopova, H. Zhu, and X. Fan, Appl. Phys. Lett. **90**, 221101 (2007).
[20]A. Watkins, J. Ward, Y. Wu, and S. N. Chormaic, Opt. Lett. **36**, 2113 (2011).
[21]H. Li, Y. Guo, Y. Sun, K. Reddy, and X. Fan, Opt. Express **18**, 25081 (2010).
[22]J. Stone, J. Opt. Soc. Am. **62**, 327 (1972).
[23]X. Fan, P. Palinginis, S. Lacey, and H. Wang, Opt. Lett. **25**, 1600 (2000).
[24]H.-M. Tzeng, K. F. Wall, M. B. Logng, and R. K. Chang, Opt. Lett. **9**, 499 (1984).
[25]H.-J. Moon, Y.-T. Chough, and K. An, Phys. Rev. Lett. **85**, 3161 (2000).
[26]S. Lacey, I. M. White, Y. Sun, S. I. Shopova, J. M. Cupps, P. Zhang, and X. Fan, Opt. Express **15**, 15523 (2007).